IET Communications

Research Article

IET Journals
The Institution of Engineering and Technology

CRB-based performance analysis of semi-blind channel estimation for massive MIMO-OFDM systems with pilot contamination

ISSN 1751-8628
Received on 20th April 2019
Revised 5th September 2019
Accepted on 16th September 2019
E-First on 15th November 2019
doi: 10.1049/iet-com.2019.0432
www.ietdl.org

Ouahbi Rekik[1] ✉, Abdelhamid Ladaycia[1], Anissa Mokraoui[1], Karim Abed-Meraim[2]

[1]*L2TI, Institut Galilée, Université Paris 13, Sorbonne Paris Cité, France*
[2]*PRISME, Université d'Orléans, France*
✉ *E-mail: ouahbi.rekik@univ-paris13.fr*

Abstract: Channel estimation, which is a key task in massive multiple-input multiple-output orthogonal-frequency division-multiplexing systems (MIMO-OFDM), is severely affected by the problem of pilot contamination during the uplink transmission. Thus, the aim of this study is to investigate, via the Cramér-Rao Bound tool, the effectiveness of semi-blind (SB) methods for pilot contamination mitigation. For synchronous cells, these analyses demonstrate the possibility to efficiently solve the pilot contamination problem, with SB approaches, when considering a finite-alphabet (non-Gaussian) communications signal. However, considering only the signal's Second Order Statistics is not enough for solving such an issue even if the SB approach is adopted. Moreover, the analyses show that it is possible to get close to the optimal performance with a SB approach even if the pilots are non-orthogonal as long as they are not fully coherent. For the asynchronous cells case, it has been demonstrated that the pilot contamination still occurs under small inter-cell delays, but can be strongly mitigated with large inter-cell delays.

1 Introduction

Massive multiple-input multiple-output (MIMO) is a promising technology for the next generation cellular networks [1]. With a higher number of base station (BS) antennas (beyond 100 antennas), compared with the classical MIMO systems, massive MIMO technology has proven its ability to improve the spectral and power efficiency [2, 3]. So that, both throughput and system capacity will be highly enhanced in order to satisfy the increasing amount of data exchange and demand for quality of service for the future cellular networks [4].

In order to fully exploit all of the potentials offered by a massive MIMO system, accurate channel state information (CSI) is necessary. It is obtained only during the uplink transmission, thanks to the channel reciprocity property and according to the widely accepted time division duplexing (TDD) protocol [4]. In that case, all users in all cells send their uplink training sequences synchronously, which are used, by the BS, to estimate the uplink channels. The traditional methods used to get the CSI rely on the pilot-based channel estimation (e.g. [1]). However, due to the non-orthogonality of the pilot sequences, these methods are severely affected by what is called *pilot contamination* [5], as depicted in Fig. 1. It is one of the major issues of massive MIMO systems that must be addressed because its effect cannot be reduced by increasing the number of BS antennas.

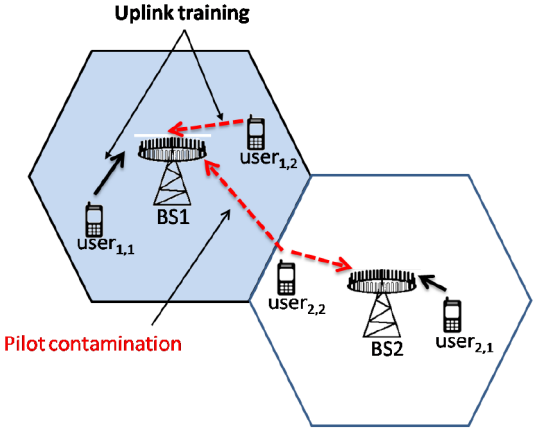

Fig. 1 *Illustration of pilot contamination in massive MIMO-OFDM systems where $user_{1,2}$ and $user_{2,2}$ (resp. $user_{1,1}$ and $user_{2,1}$) share the same training sequence*

Many pilot contamination mitigation strategies have been proposed [6–8]. Some of them propose to create more orthogonal pilots by slicing the time and frequency resources [9], however, such a choice will lead to a system capacity decrease. Other approaches are based on suppressing the inter-cell interference by appropriate signal processing techniques, based on statistical information of channel matrices [10, 11]. In such approaches, only a small portion of spatial dimensions is used for data transmission, whereas the unemployed dimensions will be used for suppressing noise and interference. However, many assumptions have to be considered to get statistical information of channel matrices. Instead of depending only on pilot sequences, a data-aided channel estimation has been considered (e.g. [12]), where the decoded data is used for channel estimation. Nonetheless, it requires perfect knowledge of the inter-cell large-scale coefficients and it is strongly assumed to have the ability to recover most of data for accurate channel estimation. Some approaches have focused on designing appropriate inter-cell communication protocols and resource allocation [13–15] in order to allow reusing pilots without inter-cell interference. The counterpart is that the information exchange among cells will add more complexity to the cellular networks.

In recent works, a particular attention has been drawn to blind (e.g. [16, 17]), and semi-blind (SB) (e.g [18, 19]) methods. The former is fully based on the statistical properties of the transmitted data, whereas the latter depends on the joint use of pilots and data.

In addition to pilot contamination mitigation techniques, many works have focused on the effect of pilot contamination, in the case of unsynchronised BSs, on the channel estimation performance [20–22].

Consequently, the focus of this paper falls into the scope of performance bounds analysis of SB channel estimation approaches under the effect of pilot contamination in the context of multi-cell massive MIMO orthogonal-frequency division-multiplexing (MIMO-OFDM) systems. The motivation for targeting SB techniques is that they allow to retain the advantages of pilot-based and blind-based approaches and hence lead to better estimation accuracy and more robustness against pilot contamination.

In [23], a brief analysis of the SB channel estimation performance bounds has been initiated in certain simplified scenarios. Here, this draft work is extended to provide a full Cramér-Rao bound (CRB)-based analysis of the pilot contamination effect and how it is mitigated in such SB context. More precisely, the main contributions are as follows:

- Unlike prior works (e.g. [18, 19]) that focused on particular estimators for either the synchronised or the unsynchronised cells cases, the current work is an estimator-independent performance analysis, where the CRB is derived for the two previous cases when considering the pilot based or the SB channel estimation. It is worth noting that a thorough study has been conducted in [24] where the achievable performance of SB approaches, compared to pilot-based ones, has been quantified for channel estimation in a single-cell MIMO-OFDM system. In the current study, a multi-cell massive MIMO-OFDM system is considered, where the phenomenon of pilot contamination is taken into account and thoroughly investigated.
- A thorough study of the channel estimation non-identifiability caused by the pilot contamination is given, leading to three propositions which describe such a phenomenon.
- The analysis has been carried out by taking into account two types of data statistics: only the Second Order Statistics (SOS) by considering a Gaussian source signal, and Higher Order Statistics (HOS) by using a finite alphabet signal. Besides, two types of pilots have been used: Zadoff-Chu sequences and randomly generated i.i.d. pilots.
- Compared to prior works [20, 22] about the unsynchronised cells case, the influence of the delay between the cell of interest and the neighbouring cells, on the pilot contamination problem, has been investigated by differentiating the effect of small delays from the one of large delays.
- In addition to the previous CRB-based theoretical study and due to the heavy computational cost of the FIM derivation, the asynchronous case has been investigated through the use of a least-squares decision feedback (LS-DF) SB channel estimator. This last analysis demonstrates that large inter-cell delays might be sufficient to mitigate the pilot contamination problem.

Practically, such performance limits analysis helps understanding the pilot contamination effect and can be exploited as a benchmark by researchers developing channel estimators for massive MIMO communications systems. Moreover, the different scenarios considered (data models, pilots models and orthogonality levels) can efficiently guide developers of communications systems for the channel estimation task.

The remainder of this paper is organised as follows. Section 2 describes the massive MIMO-OFDM system model adopted in this paper. Section 3 gives a detailed derivation of the CRB under the assumption of perfectly synchronised cells. This performance bounds analysis is used to explain how the SB approach mitigates the pilot contamination problem. The effect of pilot contamination, under the assumption of asynchronous cells, will be assessed in Section 4. This section introduces also the LS-DF estimator that will be used for numerical performance assessment. Simulation results are discussed in Section 5. Finally, Section 6 concludes the paper.

Notations

Lower case letters x represent scalars; lower case boldface letters $\boldsymbol{x}$ stand for (column) vectors; whereas matrices are represented by upper case boldface letters $\boldsymbol{X}$. Vectors' and matrices' indices represent, respectively, the cell and the receiver/transmitter that corresponds to the received/transmitted symbols. For the channel taps, the indices indicate, respectively, the cell, the transmitter and the receiver. $(\cdot)^{\mathrm{H}}$, $(\cdot)^{\mathrm{T}}$, $(\cdot)^{*}$ and $(\cdot)^{\#}$ stand, respectively, for the Hermitian, the transpose, the conjugate and the pseudo-inverse operators. $\mathrm{tr}(\cdot)$ is the trace of a matrix. $\mathrm{diag}(\boldsymbol{x})$ is a diagonal matrix with the entries of $\boldsymbol{x}$ spread along the diagonal. $\boldsymbol{I}_M$ stands for an $M \times M$ identity matrix.

2 Massive MIMO-OFDM system model

This section presents the massive MIMO-OFDM wireless system model adopted in this paper. An uplink transmission is considered. The system is composed of N_c cells each having one BS with N_r antennas and N_t randomly located users using each a single antenna.

Let's ignore at first the received signals from the adjacent cells. Therefore the received signal, after the cyclic prefix removal and FFT, at the rth BS antenna of the lth cell, assumed to be a K sub-carriers OFDM signal ($K \times 1$), is given by [25]

$$\boldsymbol{y}_{l,r} = \sum_{i=1}^{N_t} \boldsymbol{F}\, \mathscr{T}(\boldsymbol{h}_{l,i,r}) \frac{\boldsymbol{F}^{\mathrm{H}}}{K} \boldsymbol{x}_{l,i} + \boldsymbol{v}_{l,r}, \tag{1}$$

where K is the OFDM symbol length; $\boldsymbol{F}$ represents a K-point Fourier matrix; $\boldsymbol{h}_{l,i,r}$ is an $N \times 1$ vector representing the channel taps between the ith user, of the lth cell, and the rth receive antenna; $\mathscr{T}(\boldsymbol{h}_{l,i,r})$ is a circulant matrix of dimension $K \times K$ so that its first row is given by $[h_{l,i,r}(0), \boldsymbol{0}_{1\times K-N}, h_{l,i,r}(N-1), \ldots, h_{l,i,r}(1)]$ while the others are obtained by a simple cyclic shift to the right of the previous one. $\boldsymbol{x}_{l,i}$ is a vector of size $K \times 1$ which stands for the ith user OFDM symbol of cell l. $\boldsymbol{v}_{l,r}$, of size $K \times 1$, is assumed to be an additive white circulant Gaussian (CG) noise so that $E[\boldsymbol{v}_{l,r}(k)\boldsymbol{v}_{l,r}(i)^H] = \sigma^2_{v_l}\boldsymbol{I}_K\delta_{ki}$, where $\sigma^2_{v_l}$ is the noise variance at the lth cell; δ_{ki} being the Kronecker delta operator.

Using the eigenvalue decomposition of the circulant matrix $\mathscr{T}(\boldsymbol{h}_{l,i,r})$ given by

$$\mathscr{T}(\boldsymbol{h}_{l,i,r}) = \frac{\boldsymbol{F}^{\mathrm{H}}}{K} \boldsymbol{\lambda}_{l,i,r} \boldsymbol{F}, \tag{2}$$

where $\boldsymbol{\lambda}_{l,i,r}$ is a $K \times K$ diagonal matrix formed by the frequency gains of the channel at the considered subcarriers, i.e. $\boldsymbol{\lambda}_{l,i,r} = \mathrm{diag}\{\boldsymbol{W}\boldsymbol{h}_{l,i,r}\}$ and $\boldsymbol{W}$ is formed by the N first columns of $\boldsymbol{F}$, and by stacking all the data in a single vector form, the received signal, of dimension $N_rK \times 1$, at the lth BS can be re-expressed as follows:

$$\boldsymbol{y}_l = \boldsymbol{\lambda}_l \boldsymbol{x}_l + \boldsymbol{v}_l, \tag{3}$$

where $\boldsymbol{y}_l = [\boldsymbol{y}^T_{l,1} \ldots \boldsymbol{y}^T_{l,N_r}]^{\mathrm{T}}$; $\boldsymbol{x}_l = [\boldsymbol{x}^T_{l,1} \ldots \boldsymbol{x}^T_{l,N_t}]^{\mathrm{T}}$; $\boldsymbol{v}_l = [\boldsymbol{v}^T_{l,1} \ldots \boldsymbol{v}^T_{l,N_r}]^{\mathrm{T}}$; $\boldsymbol{\lambda}_l = [\boldsymbol{\lambda}_{l,1} \ldots \boldsymbol{\lambda}_{l,N_t}]$ with $\boldsymbol{\lambda}_{l,i} = [\boldsymbol{\lambda}_{l,i,1} \ldots \boldsymbol{\lambda}_{l,i,N_r}]^{\mathrm{T}}$.

In order to facilitate the derivation of the CRB w.r.t. $\boldsymbol{h}_1$, (3) is rewritten as follows:

$$\boldsymbol{y}_l = \tilde{\boldsymbol{X}}_l \boldsymbol{h}_l + \boldsymbol{v}_l, \tag{4}$$

where $\boldsymbol{h}_l = [\boldsymbol{h}^T_{l,1,1} \ldots \boldsymbol{h}^T_{l,N_t,1} \cdots \boldsymbol{h}^T_{l,1,N_r} \cdots \boldsymbol{h}^T_{l,N_t,N_r}]^{\mathrm{T}}$ is an $N_rN_tN \times 1$ vector; $\tilde{\boldsymbol{X}}_l = \boldsymbol{I}_{N_r} \otimes \boldsymbol{X}_l$ is a $N_rK \times N_rN_tN$ dimensional matrix, where $\boldsymbol{X}_l = [\boldsymbol{X}_{l,D_1}\boldsymbol{W} \cdots \boldsymbol{X}_{l,D_{N_t}}\boldsymbol{W}]$ of size $K \times N_tN$, and $\boldsymbol{X}_{l,D_i}$ is an $K \times K$ diagonal matrix containing the ith user symbols, i.e. $\boldsymbol{X}_{l,D_i} = \mathrm{diag}(\boldsymbol{x}_{l,i})$, and $\otimes$ refers to the Kronecker product.

Now, let's take into account the effect of the neighbouring cells on the first one, considered without loss of generality as the interest cell. With the assumption of perfect synchronisation between the N_c cells, (3) becomes

$$\boldsymbol{y}_1 = \sum_{l=1}^{N_c} \boldsymbol{\lambda}_l \boldsymbol{x}_l + \boldsymbol{v}_1 = \boldsymbol{\lambda}_{\mathrm{tot}} \boldsymbol{x}_{\mathrm{tot}} + \boldsymbol{v}_1, \tag{5}$$

where $\boldsymbol{\lambda}_{\mathrm{tot}} = [\boldsymbol{\lambda}_1 \cdots \boldsymbol{\lambda}_{N_c}]$ and $\boldsymbol{x}_{\mathrm{tot}} = [\boldsymbol{x}^T_1 \cdots \boldsymbol{x}^T_{Nc}]^{\mathrm{T}}$.

Similarly to (4), (5) can be rewritten as follows:

$$\boldsymbol{y}_1 = \sum_{l=1}^{N_c} \tilde{\boldsymbol{X}}_l \boldsymbol{h}_l + \boldsymbol{v}_1 = \tilde{\boldsymbol{X}}_{\mathrm{tot}} \boldsymbol{h}_{\mathrm{tot}} + \boldsymbol{v}_1, \tag{6}$$

where $\tilde{\boldsymbol{X}}_{\text{tot}} = [\tilde{\boldsymbol{X}}_1 \cdots \tilde{\boldsymbol{X}}_{N_c}]$ and $\boldsymbol{h}_{\text{tot}} = [\boldsymbol{h}_1^T \cdots \boldsymbol{h}_{N_c}^T]^{\text{T}}$.

3 Effect of pilot contamination with perfectly synchronised cells

In the following section, the effect of pilot contamination on the performance of SB channel estimation approaches is investigated, under the assumption of perfectly synchronised BSs of the different N_c cells. In such a case, and with the same pilots in all cells, the worst case of pilot contamination occurs as explained next.

3.1 Pilot contamination effect

This subsection discusses the impact of the pilot contamination in a massive MIMO-OFDM system. During the uplink data transmission, the BS has to learn the transmission channel by exploiting the known symbols (i.e. pilots) at the uplink. To adopt this strategy the pilots used within the same cell and in the neighbouring cells should be mutually orthogonal. However this necessitates a complex cell synchronisation and cooperation scheme. In addition, the channel time coherence [26, 27] limits the total number of orthogonal pilots leading to the reuse of the same pilots in many neighbouring cells. The worst case occurs when the same set of pilots is reused in all N_c adjacent cells. In this situation, (6) becomes

$$\boldsymbol{y}_1 = \sum_{l=1}^{N_c} \tilde{\boldsymbol{X}}_{1P} \boldsymbol{h}_l + \boldsymbol{v}_1 = \tilde{\boldsymbol{X}}_{1P} \sum_{l=1}^{N_c} \boldsymbol{h}_l + \boldsymbol{v}_1, \tag{7}$$

where $\tilde{\boldsymbol{X}}_{1P}$ corresponds to the pilot symbols of the first cell.

To illustrate the pilot contamination effect in that case, the least squares (*LS*) estimate of the first cell channel vector, i.e. $\boldsymbol{h}_1$, is given by:

$$\hat{\boldsymbol{h}}_1^{LS} = \tilde{\boldsymbol{X}}_{1P}^{\#} \boldsymbol{y}_1 = \boldsymbol{h}_1 + \sum_{l=1, l\neq 1}^{N_c} \boldsymbol{h}_l + \tilde{\boldsymbol{X}}_{1P}^{\#} \boldsymbol{v}_1, \tag{8}$$

with $\tilde{\boldsymbol{X}}_{1P}^{\#} = (\tilde{\boldsymbol{X}}_{1P}^{\text{H}} \tilde{\boldsymbol{X}}_{1P})^{-1} \tilde{\boldsymbol{X}}_{1P}^{\text{H}}$ is the pseudo inverse of $\tilde{\boldsymbol{X}}_{1P}$.

This equation clearly shows that the channel estimate $\hat{\boldsymbol{h}}_1^{LS}$ is affected by an additional bias corresponding to the sum of channel components of the users sharing the same pilot sequences in different cells. This phenomenon, referred to as pilot contamination, severely degrades the channel estimation performance. To overcome this problem, an alternative solution consists of using a SB channel estimation approach. In the sequel, the potential of this approach is analysed and discussed through the use of the CRB tool.

3.2 CRB derivation

Before deriving the CRB for pilot-based and SB channel estimation, it is worthwhile to remind that the CRB expresses a lower bound on the variance of any unbiased estimator. Thus, If $\hat{\boldsymbol{\theta}} = [\hat{\boldsymbol{\theta}}_1, \ldots, \hat{\boldsymbol{\theta}}_d]^{\text{T}}$ is an unbiased estimator of $\boldsymbol{\theta}$, then $\text{Cov}(\hat{\boldsymbol{\theta}}) \geq \text{CRB}(\boldsymbol{\theta})$ in the sense $\text{Cov}(\hat{\boldsymbol{\theta}}) - \text{CRB}(\boldsymbol{\theta})$ is a positive semi-definite matrix (i.e. with non-negative eigenvalues). In particular, this inequality implies that the estimation error variance of parameter $\boldsymbol{\theta}_i$ is lower bounded by the ith diagonal entry of the CRB matrix, i.e. $\text{var}(\hat{\boldsymbol{\theta}}_i) \geq \text{CRB}(\boldsymbol{\theta})_{i,i}$. In practice, such a tool provides a benchmark for unbiased estimators and alerts us to the physical impossibility of finding an estimator whose variance is less than the theoretical bound. Basically, the CRB is obtained as the inverse of the Fisher Information Matrix (FIM) [28]. The latter is denoted by $\boldsymbol{J}_{\boldsymbol{\theta\theta}}$, where $\boldsymbol{\theta}$ is the unknown deterministic parameters vector to be estimated. For the complex valued channel taps, the parameters vector $\boldsymbol{\theta}$ is defined as follows:

$$\boldsymbol{\theta} = [\boldsymbol{h}_{\text{tot}}^T (\boldsymbol{h}_{\text{tot}}^*)^T]^{\text{T}}, \tag{9}$$

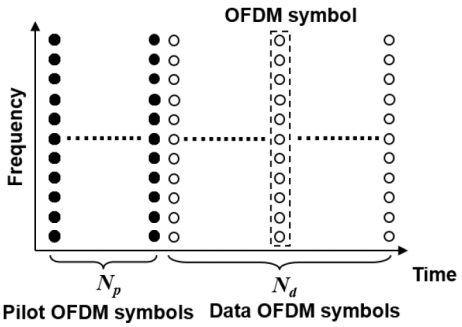

Fig. 2 *Block-type pilot arrangement*

where, for simplicity, the signal and noise powers are assumed to be known. The FIM, taking into account the pilots and data (that are statistically independent), is then expressed as follows:

$$\boldsymbol{J}_{\boldsymbol{\theta\theta}} = \boldsymbol{J}_{\boldsymbol{\theta\theta}}^p + \boldsymbol{J}_{\boldsymbol{\theta\theta}}^d, \tag{10}$$

where $\boldsymbol{J}_{\boldsymbol{\theta\theta}}^p$ is the FIM associated to the known pilots while $\boldsymbol{J}_{\boldsymbol{\theta\theta}}^d$ is related to the unknown data.

A block-type pilot arrangement, as described in Fig. 2, is adopted in this paper. In that scheme all sub-carriers are used for pilots within a specific period of time. For a pilot-based channel estimation, N_p pilot symbols will be considered. N_d i.i.d data symbols will be added to the pilots for SB approaches. Both pilots and data are assumed to be OFDM symbols of size K.

3.2.1 CRB for pilot-based channel estimation: The noise components are assumed to be independent identically distributed (i.i.d.), and only N_p pilots are used for channel estimation. Based on the data model, the pilot-based FIM can be expressed by

$$\boldsymbol{J}_{\boldsymbol{\theta\theta}}^p = \sum_{i=1}^{N_p} \boldsymbol{J}_{\boldsymbol{\theta\theta}}^{p_i}, \tag{11}$$

with $\boldsymbol{J}_{\boldsymbol{\theta\theta}}^{p_i}$ is the FIM associated to the p_ith pilot symbol.

The FIM for a complex parameter has been discussed in [29, 30], thus, it can be shown that the pilot-based FIM is given for the pilot-based channel estimation case by

$$\boldsymbol{J}_{\boldsymbol{\theta\theta}}^{p_i} = \begin{pmatrix} \boldsymbol{J}_{\boldsymbol{h}_{\text{tot}}\boldsymbol{h}_{\text{tot}}}^{p_i} & \boldsymbol{0} \\ \boldsymbol{0} & \boldsymbol{J}_{\boldsymbol{h}_{\text{tot}}^*\boldsymbol{h}_{\text{tot}}^*}^{p_i} \end{pmatrix}, \tag{12}$$

where $\boldsymbol{J}_{\boldsymbol{h}_{\text{tot}}^*\boldsymbol{h}_{\text{tot}}^*}^{p_i} = (\boldsymbol{J}_{\boldsymbol{h}_{\text{tot}}\boldsymbol{h}_{\text{tot}}}^{p_i})^*$.

By considering a massive MIMO-OFDM system with N_c cells, the pilot-based FIM associated to the channel vector $\boldsymbol{h}_{\text{tot}}$ is then expressed as follows:

$$\boldsymbol{J}_{\boldsymbol{h}_{\text{tot}}\boldsymbol{h}_{\text{tot}}}^{p_i} = \frac{\tilde{\boldsymbol{X}}_{\text{tot},p_i}^{\text{H}} \tilde{\boldsymbol{X}}_{\text{tot},p_i}}{\sigma_{\boldsymbol{v}_1}^2}, \tag{13}$$

which can also be written in a more detailed form:

$$\boldsymbol{J}_{\boldsymbol{h}_{\text{tot}}\boldsymbol{h}_{\text{tot}}}^{p_i} = \frac{1}{\sigma_{\boldsymbol{v}_1}^2} \begin{pmatrix} \tilde{\boldsymbol{X}}_{1_{p_i}}^{\text{H}} \tilde{\boldsymbol{X}}_{1_{p_i}} & \cdots & \tilde{\boldsymbol{X}}_{1_{p_i}}^{\text{H}} \tilde{\boldsymbol{X}}_{N_{cp_i}} \\ \vdots & \ddots & \vdots \\ \tilde{\boldsymbol{X}}_{N_{cp_i}}^{\text{H}} \tilde{\boldsymbol{X}}_{1_{p_i}} & \cdots & \tilde{\boldsymbol{X}}_{N_{cp_i}}^{\text{H}} \tilde{\boldsymbol{X}}_{N_{cp_i}} \end{pmatrix}. \tag{14}$$

Ideally, if the pilots of the cells are mutually orthogonal, i.e. $\tilde{\boldsymbol{X}}_{i,p_i}^{\text{H}} \tilde{\boldsymbol{X}}_{j,p_i} = \boldsymbol{0} \, \forall \, i \neq j$, then the FIM becomes a bloc diagonal matrix which is the most favourable case. On the other hand, if the cells share the same set of pilots, i.e. the worst case of pilot contamination, the FIM is then equivalent to

$$\boldsymbol{J}_{\boldsymbol{h}_{\text{tot}}\boldsymbol{h}_{\text{tot}}}^{p_i} = \frac{1}{\sigma_{\boldsymbol{v}_1}^2}\begin{pmatrix} \tilde{\boldsymbol{X}}_{1_{p_i}}^{\text{H}}\tilde{\boldsymbol{X}}_{1_{p_i}} & \dots & \tilde{\boldsymbol{X}}_{1_{p_i}}^{\text{H}}\tilde{\boldsymbol{X}}_{1_{p_i}} \\ \vdots & \ddots & \\ \tilde{\boldsymbol{X}}_{1_{p_i}}^{\text{H}}\tilde{\boldsymbol{X}}_{1_{p_i}} & \dots & \tilde{\boldsymbol{X}}_{1_{p_i}}^{\text{H}}\tilde{\boldsymbol{X}}_{1_{p_i}} \end{pmatrix}. \tag{15}$$

To compute the CRB, the FIM has to be inverted. However, according to this last equation, $\boldsymbol{J}_{\boldsymbol{h}_{\text{tot}}\boldsymbol{h}_{\text{tot}}}^{p_i}$, and consequently $\boldsymbol{J}_{\boldsymbol{h}_{\text{tot}}\boldsymbol{h}_{\text{tot}}}$, is not a full rank matrix. In fact, according to Proposition 1, the kernel of this FIM is of dimension $2(N_c-1)N_tN_rN$, corresponding to the number of indeterminacies we need to get rid of. In other words, this translates the *non-identifiability* of the channel vector of the interest cell when pilot contamination occurs.

Proposition 1: The FIM in (11) is a singular matrix and its kernel dimension is $2(N_c-1)N_tN_rN$ which corresponds to the number of indeterminacies of the problem (i.e. the number of unknown real channel parameters for the N_c-1 neighbouring cells).

Proof: The FIM kernel dimension corresponds to the number of indeterminacies we need to remove (or equivalently the number of constraints we need to consider) to achieve full identifiability.

In the case of only pilots channel estimation in the presence of pilot contamination, the only parameter vector that can be estimated without bias is $\boldsymbol{h}_{\text{tot}} = \sum_{i=1}^{N_c}\boldsymbol{h}_i$.

Now, from $\boldsymbol{h}_{\text{tot}}$ one is able to determine every single channel $\boldsymbol{h}_i, i = 1, \dots, N_c$ iff (N_c-1) channel vectors are known (besides $\boldsymbol{h}_{\text{tot}}$). Since each channel vector is complex valued and of size N_tN_rN, this corresponds to $2(N_c-1)N_tN_rN$ unknown real-valued parameters needed for full identifiability. □

3.2.2 CRB for SB channel estimation: This section is devoted to the derivation of the CRB for the SB channel estimation for a multi-cell massive MIMO-OFDM system with pilot contamination. Both pilots and data are taken into account in the derivation of the FIM as shown in (10). At first, we investigate the performance bounds of the SB scheme when only the SOS are considered. For that, a CG data model is used. Latter on, we extend this analysis to the case where information based on HOS is available. This will be illustrated by using a finite alphabet source signal.

3.2.3 Gaussian source signal: As mentioned previously, only the SOS, corresponding to the Gaussian CRB, are considered here. Hence, it is assumed that the data symbols are i.i.d. CG distributed with zero mean and a diagonal covariance matrix composed of the users' transmit powers, i.e. $\boldsymbol{C}_{\boldsymbol{x}_l} = \text{diag}(\sigma_{x_{l,i}}^2)$ with $l = 1, \dots, N_c$ and $i = 1, \dots, N_t$. Under this assumption, the received signal $\boldsymbol{y}_1$ is CG with covariance matrix

$$\boldsymbol{C}_{\boldsymbol{y}_1} = \sum_{l=1}^{N_c}\lambda_l\boldsymbol{C}_{\boldsymbol{x}_l}\boldsymbol{\lambda}_l^{\text{H}} + \sigma_{\boldsymbol{v}_1}^2\boldsymbol{I}_{KN_r}. \tag{16}$$

The data-based FIM can be expressed as follows (e.g. [31, 32]):

$$\boldsymbol{J}_{\boldsymbol{h}_{\text{tot}}\boldsymbol{h}_{\text{tot}}}^{d} = \begin{pmatrix} \boldsymbol{J}_{\boldsymbol{h}_{\text{tot}}\boldsymbol{h}_{\text{tot}}}^{d} & \boldsymbol{J}_{\boldsymbol{h}_{\text{tot}}\boldsymbol{h}_{\text{tot}}^*}^{d} \\ \boldsymbol{J}_{\boldsymbol{h}_{\text{tot}}^*\boldsymbol{h}_{\text{tot}}}^{d} & \boldsymbol{J}_{\boldsymbol{h}_{\text{tot}}^*\boldsymbol{h}_{\text{tot}}^*}^{d} \end{pmatrix}, \tag{17}$$

where $\boldsymbol{J}_{\boldsymbol{h}_{\text{tot}}\boldsymbol{h}_{\text{tot}}}^{d}$ is an $(N_cN_rN_tN)$-dimensional matrix with elements $J_{h_ih_j}^{d}$ given by the following equation:

$$J_{h_ih_j}^{d} = \text{tr}\left\{\boldsymbol{C}_{\boldsymbol{y}_1}^{-1}\frac{\partial\boldsymbol{C}_{\boldsymbol{y}_1}}{\partial h_i^*}\boldsymbol{C}_{\boldsymbol{y}_1}^{-1}\left(\frac{\partial\boldsymbol{C}_{\boldsymbol{y}_1}}{\partial h_j^*}\right)^{\text{H}}\right\}. \tag{18}$$

The ith component of the vector $\boldsymbol{h}_{\text{tot}}$ corresponds to the channel tap of indices $\{i_{N_c}, i_{N_t}, i_{N_r}, i_N\}$ associated to the cell, the user, the BS antenna and the time lag of h_i. Based on the results provided in [28], $J_{h_ih_j}^{d}$ is given by the following equation:

$$\begin{aligned} J_{h_ih_j}^{d} = (J_{h_i^*h_j^*}^{d})^* = \text{tr}\Big\{&\boldsymbol{C}_{\boldsymbol{y}_1}^{-1}\sigma_{i_{N_c},i_{N_t}}^2\boldsymbol{\lambda}_{i_{N_c},i_{N_t}}\frac{\partial\boldsymbol{\lambda}_{i_{N_c},i_{N_t}}^{\text{H}}}{\partial h_i^*} \\ &\times\boldsymbol{C}_{\boldsymbol{y}_1}^{-1}\sigma_{j_{N_c},j_{N_t}}^2\frac{\partial\boldsymbol{\lambda}_{j_{N_c},j_{N_t}}}{\partial h_j}\boldsymbol{\lambda}_{j_{N_c},j_{N_t}}^{\text{H}}\Big\} \end{aligned} \tag{19}$$

and

$$\begin{aligned} J_{h_ih_j^*}^{d} = (J_{h_i^*h_j}^{d})^* = \text{tr}\Big\{&\boldsymbol{C}_{\boldsymbol{y}_1}^{-1}\sigma_{i_{N_c},i_{N_t}}^2\boldsymbol{\lambda}_{i_{N_c},i_{N_t}}\frac{\partial\boldsymbol{\lambda}_{i_{N_c},i_{N_t}}^{\text{H}}}{\partial h_i^*} \\ &\times\boldsymbol{C}_{\boldsymbol{y}_1}^{-1}\sigma_{j_{N_c},j_{N_t}}^2\boldsymbol{\lambda}_{j_{N_c},j_{N_t}}\frac{\partial\boldsymbol{\lambda}_{j_{N_c},j_{N_t}}^{\text{H}}}{\partial h_j^*}\Big\} \end{aligned} \tag{20}$$

It is important to notice that using a SB estimation method with only the SOS of the received data is not sufficient to alleviate the pilot contamination problem. Indeed, the SOS-SB scheme reduces the number of indeterminacies but does not get rid of all of them. More precisely, we have the following proposition:

Proposition 2: The FIM in (17) is a singular matrix and, in the case $N_r > N_cN_t$, its kernel dimension is $(N_cN_t)^2$ correponding to the number of indeterminacies in the blind channel estimation case. When considering the SOS-based SB channel estimation, the kernel dimension of the FIM in (10) becomes $((N_c-1)N_t)^2$.

Proof: Considering the data only first (i.e. blind context), it is known that if the $N_r \times (N_cN_t)$ channel transfer function is irreductible, then one can estimate the channel parameters using the SOS up to an $(N_cN_t) \times (N_cN_t)$ unknown constant matrix [33, 34].

Now, since we assumed the source power known, the latter indeterminacy reduces to an unknown $(N_cN_t) \times (N_cN_t)$ unitary matrix, which can be modelled by $(N_cN_t)^2$ free real angle parameters. Somehow, the data SOS allows us to reduce the convolution model into an instantaneous (N_cN_t)-dimensional linear mixture model.

Finally, as in the only pilots case, due to the pilot contamination, the only way to complete the channel identification via the pilot use, is to have (know) the space directions of the interfering users of the neighbouring cells corresponding to $((N_c-1)N_t)^2$ real parameters to determine. □

3.2.4 Finite alphabet source signal: Here, the non-Gaussian nature of communications signals is considered through the use of a finite alphabet data model (QPSK). The observed signal at the kth sub-carrier is given by the following equation:

$$\boldsymbol{y}_{1(k)} = \boldsymbol{\lambda}_{\text{tot}_{(k)}}\boldsymbol{C}_{\boldsymbol{x}}^{\frac{1}{2}}\boldsymbol{x}_{(k)} + \boldsymbol{v}_{1(k)} \quad \text{for } k = 1, \dots, K, \tag{21}$$

where $\boldsymbol{\lambda}_{\text{tot}_{(k)}}$ is the kth Fourier component of $\boldsymbol{h}_{\text{tot}}$; $\boldsymbol{C}_{\boldsymbol{x}}$ is a block diagonal matrix formed by users' transmit powers of each cell; $\boldsymbol{x}_{(k)} = [\boldsymbol{x}_{1,(k)}^T \dots \boldsymbol{x}_{N_c,(k)}^T]^{\text{T}}$ with $\boldsymbol{x}_{l,(k)} = [x_{l,1,(k)} \dots x_{l,N_t,(k)}]^{\text{T}}$ so that $x_{l,i,(k)}$ for $k = 1, \dots, K$ are i.i.d. QPSK symbols with equal probability values.

In this case, the likelihood function is given as a sum of $Q^{N_cN_t}$ ($Q = 4$ for QPSK (4-QAM)) Gaussian pdfs as follows:

$$p(\boldsymbol{y}_{1(k)}, \boldsymbol{\theta}) = \frac{1}{Q^{N_cN_t}}\sum_{q=1}^{Q^{N_cN_t}}\frac{1}{(\pi\sigma_{\boldsymbol{v}_1}^2)^{N_r}}\text{e}^{-\|\frac{\boldsymbol{y}_{1(k)} - \boldsymbol{\lambda}_{\text{tot}_{(k)}}\boldsymbol{C}_{\boldsymbol{x}}^{\frac{1}{2}}\boldsymbol{x}_q}{\sigma_{\boldsymbol{v}_1}^2}\|}, \tag{22}$$

where $\boldsymbol{x}_q$ is the qth realisation of $\boldsymbol{x}_{(k)}$.

Consequently, the data-based FIM is a weighted sum of Gaussian FIMs given by

$$\boldsymbol{J}^{d}_{\boldsymbol{h}_{\text{tot}}\boldsymbol{h}_{\text{tot}}}(k) = \frac{1}{\sigma^2_{\boldsymbol{v}_1} Q^{N_c N_t}} \sum_{q=1}^{Q^{N_c N_t}} \left(\frac{\partial \boldsymbol{\lambda}_{\text{tot}_{(k)}} \boldsymbol{C}_{\boldsymbol{x}}^{\frac{1}{2}} \boldsymbol{x}_q}{\partial \boldsymbol{h}^*_{\text{tot}}} \right)^{\text{H}} \times \left(\frac{\partial \boldsymbol{\lambda}_{\text{tot}_{(k)}} \boldsymbol{C}_{\boldsymbol{x}}^{\frac{1}{2}} \boldsymbol{x}_q}{\partial \boldsymbol{h}^*_{\text{tot}}} \right). \tag{23}$$

To obtain a tractable FIM expression, a realistic approximation for a single-cell MIMO-OFDM system was proposed in [24]. This approximation can be easily extended to a multi-cell massive MIMO-OFDM system. To do so, let's express the elements of the data-based FIM:

$$\boldsymbol{J}^{d}_{h_i h_j}(k) = \frac{1}{\sigma^2_{\boldsymbol{v}_1} Q^{N_c N_t}} \sum_{q=1}^{Q^{N_c N_t}} \boldsymbol{x}_q^{\text{H}} \left(\frac{\partial \boldsymbol{\lambda}_{\text{tot}_{(k)}} \boldsymbol{C}_{\boldsymbol{x}}^{\frac{1}{2}}}{\partial h_i^*} \right)^{\text{H}} \times \left(\frac{\partial \boldsymbol{\lambda}_{\text{tot}_{(k)}} \boldsymbol{C}_{\boldsymbol{x}}^{\frac{1}{2}}}{\partial h_j^*} \right) \boldsymbol{x}_q . \tag{24}$$

$$\boldsymbol{J}^{d}_{h_i h_j}(k) = \frac{1}{\sigma^2_{\boldsymbol{v}_1} Q^{N_c N_t}} \sum_{q,m,l} x_q^*(m) x_q(l) \boldsymbol{\Gamma}^{i,j}_{m,l} \quad 1 \le m, l \le N_c N_t \tag{25}$$

where

$$\boldsymbol{\Gamma}^{i,j} = \left(\frac{\partial \boldsymbol{\lambda}_{\text{tot}_{(k)}} \boldsymbol{C}_{\boldsymbol{x}}^{\frac{1}{2}}}{\partial h_i^*} \right)^{\text{H}} \left(\frac{\partial \boldsymbol{\lambda}_{\text{tot}_{(k)}} \boldsymbol{C}_{\boldsymbol{x}}^{\frac{1}{2}}}{\partial h_j^*} \right).$$

Due to normalisation and QAM constellations symmetry around zero, we have

$$\begin{aligned} \frac{1}{Q^{N_t N_c}} \sum_{q=1}^{Q^{N_t N_c}} x_q^*(m) x_q(l) &= 0 \quad \text{for } m \neq l \\ \frac{1}{Q^{N_t N_c}} \sum_{q=1}^{Q^{N_t N_c}} x_q^*(m) x_q(m) &= 1 \quad \text{for } m = l \end{aligned} \tag{26}$$

Finally, the data-based FIM for the finite alphabet signals (QAM) can be reduced to:

$$\boldsymbol{J}^{d}_{h_i h_j}(k) = \frac{1}{\sigma^2_{\boldsymbol{v}}} \text{tr}\left\{ \boldsymbol{\Gamma}^{i,j} \right\} \tag{27}$$

The total data-based FIM is then obtained as follows:

$$\boldsymbol{J}^{d}_{\boldsymbol{h}_{\text{tot}}\boldsymbol{h}_{\text{tot}}} = N_d \sum_{k=1}^{K} \boldsymbol{J}^{d}_{\boldsymbol{h}_{\text{tot}}\boldsymbol{h}_{\text{tot}}}(k), \tag{28}$$

where N_d is the total number of data symbols.

Remark 1: Even though the proposed FIM simplification applies for any symmetric finite alphabet signal, the accuracy of the approximation decreases with the constellation order level and would be valid only for high SNRs in such a case.

Thanks to the implicit HOS information available in this non-Gaussian case, the SB-based channel estimation is able to alleviate completely the pilot contamination problem according to the following proposition:

Proposition 3: The non-Gaussian SB FIM as given in (10) is non-singular meaning that all indeterminacies have been removed.

Proof: For non-Gaussian (communications) signals, the information provided by the SOS as well as HOS of the data allows us to identify the channels up to an unknown $(N_c N_t) \times (N_c N_t)$ diagonal unitary matrix (see, e.g. identifiability results in [35]). This corresponds to $N_c N_t$ unknown real parameters that can be easily estimated through the use of the pilots. □

In this case, the top-left $(N_r N_t N) \times (N_r N_t N)$ block of the FIM inverse is considered as the CRB for the SB estimation of the first cell channel vector.

4 Effect of pilot contamination with unsynchronised cells

This section is devoted to the effect of pilot contamination on the performance of SB channel estimation approaches, when the BSs in the different N_c cells are not synchronised. Such an assumption is more realistic and practical for the cellular network. It is shown in [20, 21], that this desynchronisation might help mitigating the pilot contamination problem. Here, this issue is analysed in detail and it is shown, in particular, that under certain conditions detailed below (small inter-cell delays) the pilot contamination still occurs for asynchronous MIMO-OFDM systems. For large inter-cell delays, the pilot contamination problem might be mitigated where this case is investigated through the CRB derivation, by considering the adjacent cells signal together with the AWGN noise as a coloured noise. These results will be experimentally supported by an estimator-dependent study, based on a LS-DF estimator.

4.1 Small inter-cell delay case

This subsection provides an explanation on why the pilot contamination problem persists when the inter-cell delays are small. Indeed, without lose of generality, consider two time-domain OFDM signals, sent from two adjacent cells using the same pilot sequence, and received at one BS antenna

$$z_1(t) = h_1(t) * x_{\text{CP},1}(t) \tag{29}$$

$$z_2(t) = h_2(t) * x_{\text{CP},1}(t-\tau) = h_2(t-\tau) * x_{\text{CP},1}(t) \tag{30}$$

$x_{\text{CP},1}(t)$ being the sequential OFDM signal in the time domain including the cyclic prefix (CP), $*$ is the convolution operator and τ is introduced here to model the inter-cell delay. Hence, when the signal from cell 1 is corrupted by the one from cell 2, one observes

$$z(t) = z_1(t) + z_2(t) = (h_1(t) + h_2(t-\tau)) * x_{\text{CP},1}(t) \tag{31}$$

Consequently, if the channel size N and the delay τ are such that

$$\tau + N \le L + 1 \tag{32}$$

L being the CP length, the model given in (31) coincides with the one in (7), which shows that the pilot contamination problem remains unsolved in this case, which might represent a 'rough synchronisation' context. This situation is illustrated by the simulation results in Fig. 3.

4.2 Large inter-cell delay case

Now, an effective channel estimation becomes possible in this case (see, e.g. [22]) and to analyse it in the sequel, the pilots from the neighbouring cells are considered as interference signal where the interference and the noise term will be modelled as a coloured Gaussian signal $\boldsymbol{v}_{\text{col}}$ independent from the signals of the cell of interest. The noise vector is assumed to be of zero mean and unknown covariance matrix $\boldsymbol{C}_{\text{v}}$, so that the received signal model becomes

$$\boldsymbol{y}_1 = \tilde{\boldsymbol{X}}_1 \boldsymbol{h}_1 + \boldsymbol{v}_{\text{col}} . \tag{33}$$

When sending only known pilots, the received signal is so that $\boldsymbol{y}_1 \sim \mathcal{N}(\boldsymbol{\mu}_{\boldsymbol{y}_1}(\boldsymbol{\theta}) = \tilde{\boldsymbol{X}}_{1_p} \boldsymbol{h}_1, \boldsymbol{C}_{\boldsymbol{y}_1}(\boldsymbol{\theta}) = \boldsymbol{C}_{\boldsymbol{v}})$. The parameters vector to be estimated is expressed as follows:

$$\boldsymbol{\theta} = [\boldsymbol{h}_1^T (\boldsymbol{h}_1^*)^T \boldsymbol{q}^T (\boldsymbol{q}^*)^T]^{\text{T}}, \tag{34}$$

where $\boldsymbol{h}_1$, of size $N_r N_t N$, is the vector of the channel components of the cell of interest, $\boldsymbol{q} = [q_1, q_2, \ldots, q_{N_q}]^{\mathrm{T}}$, where $q_i, i = 1, \ldots, N_q$ are the parameters used to represent the covariance matrix $\boldsymbol{C}_v$.

According to the complex representation of $\boldsymbol{\theta}$, the global pilot-based FIM is given by

$$\boldsymbol{J}^p_{\boldsymbol{\theta\theta}} = \begin{pmatrix} \boldsymbol{J}^p_{\boldsymbol{h}_1\boldsymbol{h}_1} & \boldsymbol{J}^p_{\boldsymbol{h}_1\boldsymbol{h}_1^*} & \boldsymbol{J}^p_{\boldsymbol{h}_1\boldsymbol{q}} & \boldsymbol{J}^p_{\boldsymbol{h}_1\boldsymbol{q}^*} \\ \boldsymbol{J}^p_{\boldsymbol{h}_1^*\boldsymbol{h}_1} & \boldsymbol{J}^p_{\boldsymbol{h}_1^*\boldsymbol{h}_1^*} & \boldsymbol{J}^p_{\boldsymbol{h}_1^*\boldsymbol{q}} & \boldsymbol{J}^p_{\boldsymbol{h}_1^*\boldsymbol{q}^*} \\ \boldsymbol{J}^p_{\boldsymbol{q}\boldsymbol{h}_1} & \boldsymbol{J}^p_{\boldsymbol{q}\boldsymbol{h}_1^*} & \boldsymbol{J}^p_{\boldsymbol{q}\boldsymbol{q}} & \boldsymbol{J}^p_{\boldsymbol{q}\boldsymbol{q}^*} \\ \boldsymbol{J}^p_{\boldsymbol{q}^*\boldsymbol{h}_1} & \boldsymbol{J}^p_{\boldsymbol{q}^*\boldsymbol{h}_1^*} & \boldsymbol{J}^p_{\boldsymbol{q}^*\boldsymbol{q}} & \boldsymbol{J}^p_{\boldsymbol{q}^*\boldsymbol{q}^*} \end{pmatrix}. \tag{35}$$

Their elements are derived according to the general Gaussian CRB derivation model

$$\begin{aligned} J^p_{\theta_i\theta_j} = &\left\{\frac{\partial \boldsymbol{\mu}_{\boldsymbol{y}_1}(\boldsymbol{\theta})}{\partial \theta_i^*}\right\}^{\mathrm{H}} \boldsymbol{C}^{-1}_{\boldsymbol{y}_1}(\boldsymbol{\theta})\left\{\frac{\partial \boldsymbol{\mu}_{\boldsymbol{y}_1}(\boldsymbol{\theta})}{\partial \theta_j^*}\right\} \\ &+\mathrm{tr}\left\{\boldsymbol{C}^{-1}_{\boldsymbol{y}_1}(\boldsymbol{\theta})\frac{\partial \boldsymbol{C}_{\boldsymbol{y}_1}(\boldsymbol{\theta})}{\partial \theta_i^*}\boldsymbol{C}^{-1}_{\boldsymbol{y}_1}(\boldsymbol{\theta})\left(\frac{\partial \boldsymbol{C}_{\boldsymbol{y}_1}(\boldsymbol{\theta})}{\partial \theta_j^*}\right)^{\mathrm{H}}\right\}. \end{aligned} \tag{36}$$

Given (33), it can be shown that

$$\frac{\partial \boldsymbol{\mu}_{\boldsymbol{y}_1}(\boldsymbol{\theta})}{\partial \boldsymbol{h}_1} = \tilde{\boldsymbol{X}}_{1_p}, \quad \frac{\partial \boldsymbol{\mu}_{\boldsymbol{y}_1}(\boldsymbol{\theta})}{\partial \boldsymbol{h}_1^*} = \boldsymbol{0}, \quad \frac{\partial \boldsymbol{\mu}_{\boldsymbol{y}_1}(\boldsymbol{\theta})}{\partial \boldsymbol{q}} = \boldsymbol{0}, \quad \frac{\partial \boldsymbol{\mu}_{\boldsymbol{y}_1}(\boldsymbol{\theta})}{\partial \boldsymbol{q}^*} = \boldsymbol{0}$$

$$\frac{\partial \boldsymbol{C}_{\boldsymbol{y}_1}(\boldsymbol{\theta})}{\partial \boldsymbol{h}_1} = \boldsymbol{0}, \quad \frac{\partial \boldsymbol{C}_{\boldsymbol{y}_1}(\boldsymbol{\theta})}{\partial \boldsymbol{h}_1^*} = \boldsymbol{0}.$$

Consequently, the FIM, for the pilot-based case, will be expressed as follows:

$$\boldsymbol{J}^p_{\boldsymbol{\theta\theta}} = \begin{pmatrix} \tilde{\boldsymbol{X}}^{\mathrm{H}}_{1_p}\boldsymbol{C}_{\boldsymbol{v}}^{-1}\tilde{\boldsymbol{X}}_{1_p} & \boldsymbol{0} & \boldsymbol{0} & \boldsymbol{0} \\ \boldsymbol{0} & \tilde{\boldsymbol{X}}^{T}_{1_p}(\boldsymbol{C}_{\boldsymbol{v}}^{-1})^*\tilde{\boldsymbol{X}}^*_{1_p} & \boldsymbol{0} & \boldsymbol{0} \\ \boldsymbol{0} & \boldsymbol{0} & \boldsymbol{J}^p_{\boldsymbol{q}\boldsymbol{q}} & \boldsymbol{0} \\ \boldsymbol{0} & \boldsymbol{0} & \boldsymbol{0} & \boldsymbol{J}^p_{\boldsymbol{q}^*\boldsymbol{q}^*} \end{pmatrix}. \tag{37}$$

Finally, the pilot-based CRB for the channel parameter vector is given by the following equation:

$$\mathrm{CRB}_{\mathrm{OP}} = \mathrm{tr}\{(\tilde{\boldsymbol{X}}^{\mathrm{H}}_{1_p}\boldsymbol{C}_{\boldsymbol{v}}^{-1}\tilde{\boldsymbol{X}}_{1_p})^{-1}\}. \tag{38}$$

By taking into account the known pilots and the unknown data, the SB FIM is given by (10). Moreover, by assuming known transmit powers, the vector of parameters to be estimated is given by (34), whereas the global data-based FIM is given by the following equation:

$$\boldsymbol{J}^d_{\boldsymbol{\theta\theta}} = \begin{pmatrix} \boldsymbol{J}^d_{\boldsymbol{h}_1\boldsymbol{h}_1} & \boldsymbol{J}^d_{\boldsymbol{h}_1\boldsymbol{h}_1^*} & \boldsymbol{J}^d_{\boldsymbol{h}_1\boldsymbol{q}} & \boldsymbol{J}^d_{\boldsymbol{h}_1\boldsymbol{q}^*} \\ \boldsymbol{J}^d_{\boldsymbol{h}_1^*\boldsymbol{h}_1} & \boldsymbol{J}^d_{\boldsymbol{h}_1^*\boldsymbol{h}_1^*} & \boldsymbol{J}^d_{\boldsymbol{h}_1^*\boldsymbol{q}} & \boldsymbol{J}^d_{\boldsymbol{h}_1^*\boldsymbol{q}^*} \\ \boldsymbol{J}^d_{\boldsymbol{q}\boldsymbol{h}_1} & \boldsymbol{J}^d_{\boldsymbol{q}\boldsymbol{h}_1^*} & \boldsymbol{J}^d_{\boldsymbol{q}\boldsymbol{q}} & \boldsymbol{J}^d_{\boldsymbol{q}\boldsymbol{q}^*} \\ \boldsymbol{J}^d_{\boldsymbol{q}^*\boldsymbol{h}_1} & \boldsymbol{J}^d_{\boldsymbol{q}^*\boldsymbol{h}_1^*} & \boldsymbol{J}^d_{\boldsymbol{q}^*\boldsymbol{q}} & \boldsymbol{J}^d_{\boldsymbol{q}^*\boldsymbol{q}^*} \end{pmatrix}. \tag{39}$$

Note that the received data signal satisfies $\boldsymbol{y}_1 \sim \mathcal{N}(\boldsymbol{\mu}_{\boldsymbol{y}_1}(\boldsymbol{\theta}) = \boldsymbol{0}, \boldsymbol{C}_{\boldsymbol{y}_1}(\boldsymbol{\theta}) = \boldsymbol{\lambda}_1\boldsymbol{C}_{\boldsymbol{x}_1}\boldsymbol{\lambda}_1^{\mathrm{H}} + \boldsymbol{C}_{\boldsymbol{v}})$.

Unfortunately, in that case, the off diagonal blocks $\boldsymbol{J}^d_{\boldsymbol{h}_1\boldsymbol{q}}$ and $\boldsymbol{J}^d_{\boldsymbol{h}_1\boldsymbol{q}^*}$ are not equal to zero as in the pilot-based case, and hence the channel estimation CRB depends on the estimation of the vector $\boldsymbol{q}$. The proper parameterisation of the interference plus noise covariance matrix being quite challenging, we propose next to investigate the performance of the SB case in this cell asynchronous context by using an estimator-dependent analysis.

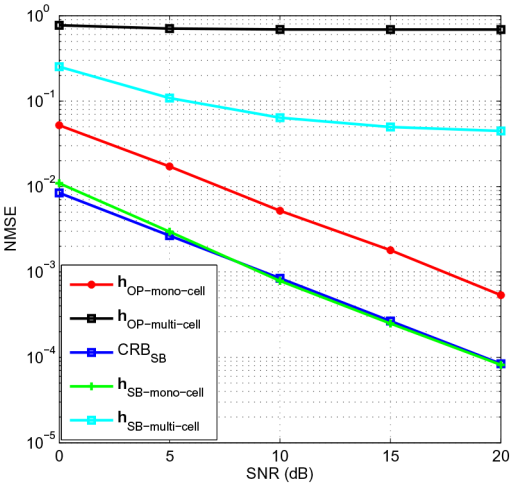

Fig. 3 *NMSE of LS and LS-DF estimators versus SNR with small inter-cell delays*

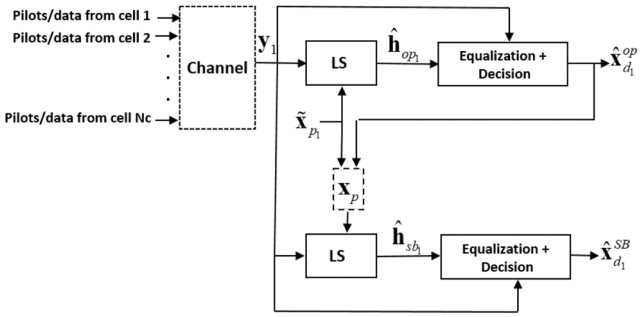

Fig. 4 *LS-DF SB channel estimation approach*

Remark 2: Note that, the pilots of the cell of interest are known and hence they are considered as deterministic. Therefore, in the case where neighbouring cells share the same pilots, the randomness comes only from the unknown data and noise terms. In such a case, the statistical independence assumption is valid. However, the i.i.d. coloured Gaussian model remains a limiting approximation. In addition to that, a main difficulty comes from the 'non-synchronisation' of the cells, which makes the data model of the signals impinging from adjacent cells quite complex (we cannot rely on the simple OFDM model in (3) obtained after CP removal and FFT) and consequently the exact FIM derivation becomes cumbersome and numerically unattractive.

4.3 LS-DF estimator performance analysis

The derivation and performance of the LS-DF estimator, introduced in [36], are presented in this section. This 'relatively simple' estimator is used to illustrate the SB performance in the different contexts of cell desynchronisation, discussed previously.

Traditionally used for data equalisation, the LS-DF algorithm is defined as an LS estimator which incorporates a feedback equaliser. During the LS-DF process, the estimated data are re-injected, as a feedback, to the equalisation step in order to enhance the estimation performance of the transmitted data. This process can be iterated several times for more accuracy.

We have exploited this method as a SB channel estimator in [36], where the estimated data are considered as extra 'pilots' for the channel taps estimation. The use of LS-DF estimator, as a SB approach, for massive MIMO channel identification is illustrated in Fig. 4 and resumed by the following steps:

• A pilot-based channel estimation is performed using the conventional LS estimator as follows:

$$\hat{\boldsymbol{h}}_{op_1} = \left(\tilde{\boldsymbol{X}}^{\mathrm{H}}_{1_p}\tilde{\boldsymbol{X}}_{1_p}\right)^{-1}\tilde{\boldsymbol{X}}^{\mathrm{H}}_{1_p}\boldsymbol{y}_1, \tag{40}$$

where $\tilde{\boldsymbol{X}}_{1_p}$ is as defined in (7).

• A zero-forcing (ZF) equaliser is used to estimate the transmitted data, by applying the inverse of the channel frequency response to the received signal as follows:

$$\boldsymbol{x}_{zf} = \hat{\boldsymbol{\lambda}}^{\#} \boldsymbol{y}_1, \tag{41}$$

where $\hat{\boldsymbol{\lambda}}$ is obtained from the channel frequency response of $\hat{\boldsymbol{h}}_{op_1}$ and $\boldsymbol{x}_{zf}$ is the equalised signal.

• A hard decision is performed on the equalised signal to obtain the estimate of the transmitted signal $\hat{\boldsymbol{x}}_{d_1}^{op}$.

• An LS estimator is then applied using the new training sequences (i.e. pilots) given by $\boldsymbol{x}_p = [\tilde{\boldsymbol{x}}_{1_p}^T \ (\boldsymbol{C}_{\boldsymbol{x}_1}^{\frac{1}{2}} \hat{\boldsymbol{x}}_{d_1}^{op})^T]^T$, where $\boldsymbol{C}_{\boldsymbol{x}_1}$ is the known transmit data power matrix introduced in (21). This step will lead to the SB channel estimate $\hat{\boldsymbol{h}}_{sb_1}$.

• A ZF equaliser, followed by a hard decision are performed to obtain the SB estimate of the transmitted data $\hat{\boldsymbol{x}}_{d_1}^{\mathrm{SB}}$.

The LS channel estimation performance has been widely discussed in literature, where it has been shown that the mean squares error (MSE) of this estimator reaches the $\mathrm{CRB}_{\mathrm{OP}}$ in a single cell system with AWGN noise. Therefore the $\mathrm{MSE}_{\mathrm{OP}}$ is then given by the following equation:

$$\mathrm{MSE}_{\mathrm{OP}} = \mathrm{CRB}_{\mathrm{OP}} = \sigma_{v_1}^2 tr\left\{\left(\tilde{\boldsymbol{X}}_{1_p}^{\mathrm{H}} \tilde{\boldsymbol{X}}_{1_p}\right)^{-1}\right\}. \tag{42}$$

However, in a multi-cell system, the effect of the adjacent cells signals will result in an extra bias term of inter-cell interference which will affect the estimation performance, depending on the inter-cell delay range. In that case, the LS-DF performance would be affected as well as can be seen in Figs. 3 and 5.

5 Performance analysis and discussions

In the following section, numerical experiments will be performed to highlight the different results given in the previous sections. The pilots are generated according to Zadoff-Chu sequences [37]. The $N_c N_t N_r N$ channel coefficients are all generated using i.i.d. unit-power, zero-mean, Gaussian distribution. It is important to note that the average signal-to-noise ratio (SNR) is calculated based on the received signal $\boldsymbol{y}_1$ given in (5), i.e. $\mathrm{SNR} = E(\| \boldsymbol{\lambda}_{\mathrm{tot}} \boldsymbol{x}_{\mathrm{tot}} \|^2)/E(\| \boldsymbol{v}_1 \|^2) = \mathrm{tr}(\boldsymbol{\lambda}_{\mathrm{tot}} \boldsymbol{C}_{\boldsymbol{x}} \otimes \boldsymbol{I}_K \boldsymbol{\lambda}_{\mathrm{tot}}^{\mathrm{H}})/(N_r K \sigma_v^2)$. Moreover, the differences in users powers reflect their random locations. The different simulation parameters are summarised in Table 1, unless otherwise mentioned.

5.1 Perfectly synchronised BSs

This section discusses the potential of the SB channel estimation approaches, when the worst case of pilot contamination occurs in a massive MIMO-OFDM system.

Experiment 1: Fig. 6 illustrates the normalised CRB for the channel parameters vector $\boldsymbol{h}_1$, given by $\mathrm{tr}\{\mathrm{CRB}\}/\| \boldsymbol{h}_1 \|^2$, for SB channel estimation with respect to the SNR for QPSK model as well as the Gaussian (G) data model using orthogonal pilots. A comparison is made with respect to the pilot-based $\mathrm{CRB}_{\mathrm{OP}}^{\mathrm{O}}$ case, which is the top-left block of the inverse of the FIM given in (14), using orthogonal (O) intra and inter-cell pilots. Note that $\mathrm{CRB}_{\mathrm{OP}}^{\mathrm{NO}}$ and $\mathrm{CRB}_{\mathrm{SB}}^{\mathrm{G-NO}}$ for the non-orthogonal case (when the adjacent cells use the same pilots) are not considered since, as mentioned in Sections 3.2.1 and 3.2.3, the channel parameters vector of the interest cell cannot be identified in that cases. However, such an ambiguity is removed by SB techniques for finite alphabet source signals as illustrated by the plot of $\mathrm{CRB}_{\mathrm{SB}}^{\mathrm{QPSK-NO}}$, which is obtained from the FIM given in (23) and stands for the SB CRB of a QPSK signal for the worst case of non orthogonal (NO) pilots (i.e. adjacent cells using the same pilots). As can be seen, $\mathrm{CRB}_{\mathrm{SB}}^{\mathrm{QPSK-NO}}$ is almost superposed with $\mathrm{CRB}_{\mathrm{SB}}^{\mathrm{QPSK-O}}$, which denotes the case of orthogonal pilots. Ideally, the latter CRB can be obtained by ignoring the adjacent cells (i.e. $N_c = 1$).

Since the effect of pilot contamination is due to signals from adjacent cells, as described in Section 3.1, Fig. 7 illustrates the scenario of Fig. 6 but with a higher number of cells (here the cell of interest is surrounded by six cells). One can observe that the previous results still hold under severe conditions of pilot contamination.

Experiment 2: Now, the impact of pilots orthogonality level is investigated through the following metric:

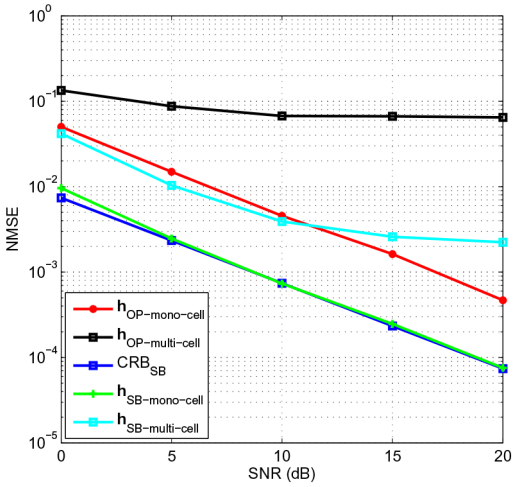

Fig. 5 *NMSE of LS and LS-DF estimators versus SNR with large inter-cell delays*

Table 1 Simulation parameters

Parameters	Specifications
number of cells	$N_c = 3$
number of receive antennas	$N_r = 100$
number of users per cell	$N_t = 2$
channel taps	$N = 4$
number of OFDM sub-carriers	$K = 64$
number of OFDM pilot symbols	$N_p = 4$
number of OFDM data symbols	$N_d = 40$
N_c pilot signal powers, dBm	$P_{x_p} = [23\ 18\ 15]$
$(N_t) \times N_c$ data signal powers, dBm	$P_{x_d} = [(20\ 18.8),$ (15.7 13.3), (11.2 9.1)]

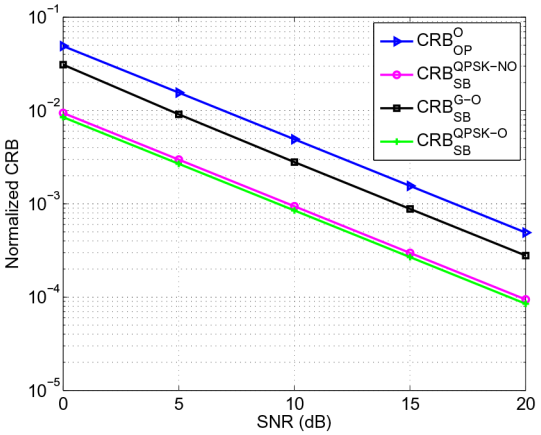

Fig. 6 *Normalised CRB versus SNR*

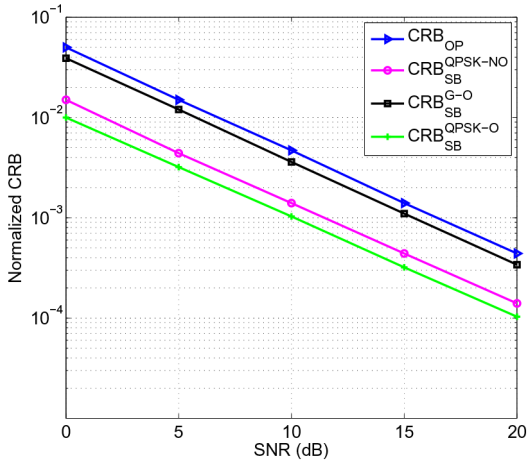

Fig. 7 *Normalised CRB versus SNR with six adjacent cells*

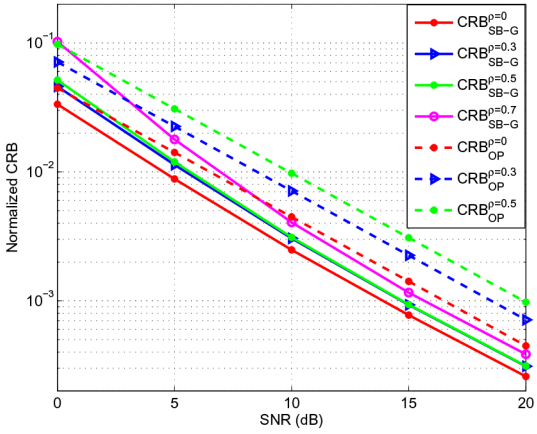

Fig. 8 *Gaussian CRB versus SNR with different orthogonality levels*

$$\rho = \frac{\| \tilde{\boldsymbol{X}}_{i_P}^{\mathrm{H}} \tilde{\boldsymbol{X}}_{j_P} \|}{\| \tilde{\boldsymbol{X}}_{i_P} \| \| \tilde{\boldsymbol{X}}_{j_P} \|}, \tag{43}$$

where $\| \cdot \|$ is the 2-norm.

Note that $0 \leq \rho \leq 1$, so that $\rho = 0$ corresponds to the perfect orthogonality, whereas $\rho = 1$, corresponding to fully-coherent training sequences, stands for the worst case of pilot contamination, i.e. same synchronised pilots.

As can be expected, in the case of non-perfectly orthogonal pilots, the channel vector estimation is slightly degraded but even with a high level of non orthogonality ($\rho = 70\%$ for the SB case and $\rho = 50\%$ for the OP case), the channel estimation for the OP and the Gaussian cases remains possible with relatively good estimation accuracy for moderate and high SNRs as illustrated in Fig. 8.

Experiment 3: In order to further investigate the impact of the pilots structure on the pilot contamination, i.i.d. Gaussian distributed pilots are considered in this experiment. As given in Fig. 9, $\mathrm{CRB}_{\mathrm{SB}}^{\mathrm{G-multi\text{-}cell}}$ described in Section 3.2.3 (respectively, $\mathrm{CRB}_{\mathrm{SB}}^{\mathrm{QPSK-multi\text{-}cell}}$ described in Section 3.2.4) is almost superposed to $\mathrm{CRB}_{\mathrm{SB}}^{\mathrm{G-mono\text{-}cell}}$ (respectively, $\mathrm{CRB}_{\mathrm{SB}}^{\mathrm{QPSK-mono\text{-}cell}}$), which indicates that the pilot contamination no longer persists and, thus, it is possible to use only SOS for SB channel estimation. Besides, a pilot-based is now possible as given by $\mathrm{CRB}_{\mathrm{OP}}^{\mathrm{multi\text{-}cell}}$ but with a degradation compared to the mono-cell case $\mathrm{CRB}_{\mathrm{OP}}^{\mathrm{mono\text{-}cell}}$, given by (42), due to the interference terms from the neighbouring cells. Actually, the independent pilots are different but not perfectly orthogonal which refers to the same results announced in *experiment 2* but given in terms of the orthogonality level.

Experiment 4: By considering the worst scenario of pilot contamination, the effect of the number of OFDM data symbols, i.e. N_d, on the $\mathrm{CRB}_{\mathrm{SB}}^{\mathrm{QPSK-NO}}$, for a given SNR = 10 dB, is illustrated in Fig. 10. It can be observed that, starting by one OFDM data symbol, the BS can successfully identify and estimate the channel components of the interest cell. Moreover, the CRB is significantly lowered with just a few tens of OFDM data symbols and almost reaches the performance of the orthogonal case, i.e. $\mathrm{CRB}_{\mathrm{SB}}^{\mathrm{QPSK-O}}$. Such a result matches perfectly with the limited coherence time constraint of massive MIMO systems and helps to reduce the computational cost. As compared to $\mathrm{CRB}_{\mathrm{OP}}^{\mathrm{O}}$ a significant performance gain in favour of the SB method is noticed.

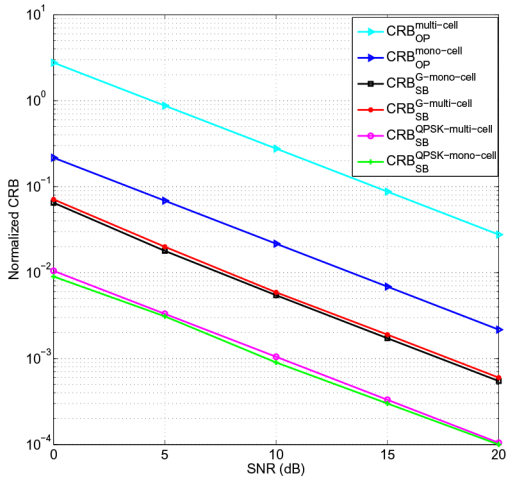

Fig. 9 *Normalised CRB versus SNR with i.i.d. pilots*

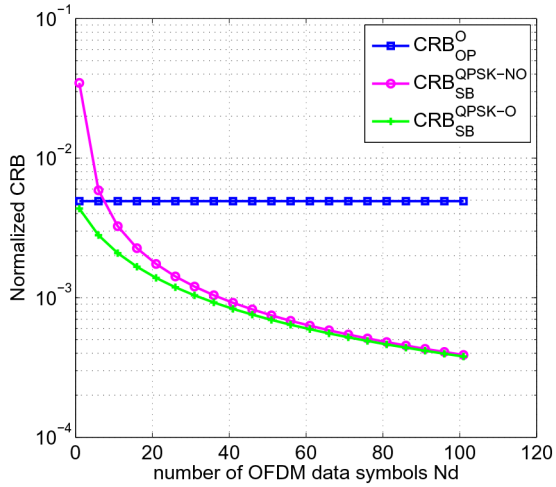

Fig. 10 *Normalised CRB versus number of OFDM data symbols N_d*

Experiment 5: By considering again the worst case of pilot contamination, the behaviour of the CRBs considered in Fig. 6, with respect to the number of BS antennas, i.e. N_r, is investigated in Fig. 11. It is easily observed that when N_r increases, which leads also to the increase of the number of channel components to be estimated, the $\mathrm{CRB}_{\mathrm{SB}}^{\mathrm{QPSK}}$ is significantly lowered thanks to the increased receive diversity. Such a result supports the effectiveness of SB techniques for pilot contamination mitigation in the context of massive MIMO-OFDM systems.

Experiment 6: The channel order is often not known with accuracy and needs extra processing for its estimation. Thus, in Fig. 12, we investigate the behaviour of the aforementioned performance when the number of the channel taps is overestimated, i.e. considered equal to its maximum value corresponding to the CP size ($N = L$). For illustration purpose, we have considered two cells, each with one user and a BS with $N_r = 10$ antennas. As can be seen from Fig. 12, the channel order overestimation leads to a performance loss of ~6 dB which corresponds to the ratio (in dB) between the overestimated and the exact channel orders.

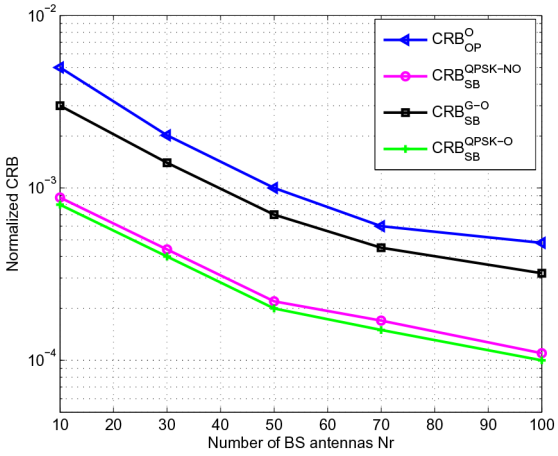

Fig. 11 *Normalised CRB versus number of BS antennas N_r*

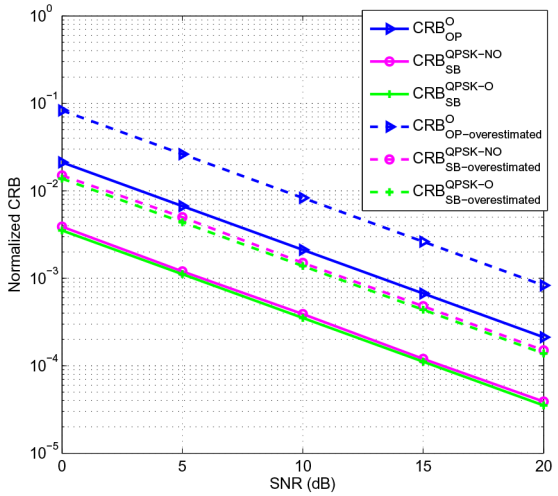

Fig. 12 *Normalised CRB versus SNR with channel order overestimation*

5.2 Unsynchronised BSs

This section investigates the SB channel estimation potential in the case of unsynchronised BSs. The non-synchronisation was generated by using the same pilots in all N_c cells but with different time delays compared to the target cell. Data symbols are assumed to be drawn from a finite alphabet signal (QPSK).

Experiment 7: Fig. 3 illustrates the NMSE of the LS estimator, as a pilot-based one, and the LS-DF estimator, as a SB approach, with respect to the SNR, in the case of small inter-cell delays. As explained in Section 4.1 and as given in the aforementioned figure, with small inter-cell delays, the problem of pilot contamination is still unsolved. For comparison, the results corresponding to the mono-cell case are also provided in this figure. In particular, the latter highlights the effectiveness of the LS-DF estimator (which reaches the CRB) in the absence of pilot contamination.

Experiment 8: Fig. 5 investigates the performance, through the NMSE, of the LS-DF estimator, as a SB approach, in the case of large inter-cell delays. Compared to the small inter-cell case, the performance is slightly improved in this context. For only pilot (OP) case with unsynchronised cells, it is possible to identify and estimate the channel components of the interest cell with a moderate estimation error. As expected, the SB case, described by $\boldsymbol{h}_{\mathrm{SB-multi-cell}}$, outperforms the OP case, but with a degradation compared to the case of perfectly orthogonal pilots $\boldsymbol{h}_{\mathrm{SB-mono-cell}}$, which has a near optimal performance as it is almost superposed to the lower bound given by $\mathrm{CRB}_{\mathrm{SB}}$.

Experiment 9: Fig. 13 investigates the effect of the pilots' structure on the performance of the LS-DF estimator, by using

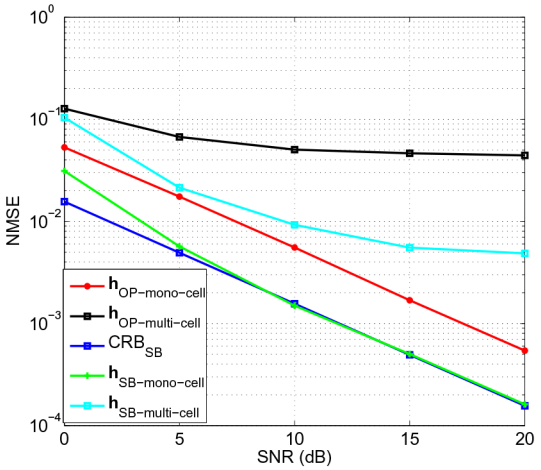

Fig. 13 *NMSE of LS and LS-DF estimators versus SNR with i.i.d. pilots*

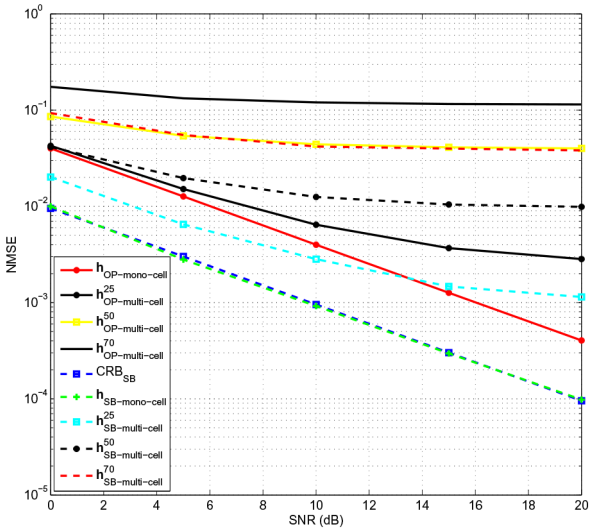

Fig. 14 *NMSE of LS and LS-DF estimators versus SNR with different data powers*

randomly generated i.i.d. pilots. The performances obtained are similar to those obtained in the case of large inter-cell delays.

Experiment 10: Since the signal power of users in the adjacent cells is usually less than the signal power of users in the cell of interest, the effect of such a parameter, on the LS-DF performance, is investigated in Fig. 14. We have considered the system parameters of Table 1 but, for each cell the N_t users are given the same power. The superscript stands for the ratio (in percentage) between each neighbouring cell users power and the interest cell users power. One can observe, for example that, for an interference level of 25% (corresponding approximately to 50% interference level if we add the interference terms of the two neighbouring cells), the channel estimation for low and moderate SNRs with the SB approach ($\boldsymbol{h}^{25}_{\mathrm{SB-multi-cell}}$) is better than the one with the interference-free OP approach ($\boldsymbol{h}_{\mathrm{OP-mono-cell}}$).

6 Conclusion

This paper focused on the performance bounds analysis of SB channel estimation approaches, under the effect of pilot contamination, for multi-cell massive MIMO-OFDM systems. An estimator-independent analysis has been conducted on the basis of the CRB by considering, at first, the worst case of pilot contamination for different data models, then, by taking into account unsynchronised BSs. It has been shown that the pilot contamination issue introduces a non-identifiability of the channel vector of the interest cell, which is not fully solved by considering only SOS, unless using non-perfectly orthogonal pilots, but can be

efficiently solved with finite alphabet signals. Moreover, interesting performance is obtained with just small numbers of data symbols, which matches with the short coherence time constraint in massive MIMO-OFDM systems and allows the use of more data for throughput improving.

On the other hand, under the assumption of unsynchronised BSs with small inter-cell delays, the problem of pilot contamination remains unsolved. However, large inter-cell delays can allow to mitigate the pilot based non-identifiability issue. It is worth pointing out that, under this assumption, the coloured Gaussian model is a limiting approximation. Besides, the 'non-synchronisation' of the cells makes the data model of the signals impinging from adjacent cells quite complex and consequently the exact FIM derivation becomes cumbersome and numerically unattractive. Another important result of this study is that, instead of using perfectly orthogonal pilots, which limits the number of potential users, it is possible to design and use non-orthogonal pilots with moderate non-orthogonality levels, which helps increasing the number of potential users, without much affecting the channel estimation quality. Such a result, along with efficient SB channel estimator design, can be considered for potential future works.

7 References

[1] Marzetta, T.L.: 'Noncooperative cellular wireless with unlimited numbers of base station antennas', *IEEE Trans. Wirel. Commun.*, 2010, **9**, (11), pp. 3590–3600

[2] Zhang, X., Wu, S., Yu, S., *et al.*: 'Spectral efficiency of massive MIMO networks with pilot contamination and channel covariance matrix estimation', *IET Commun.*, 2018, **13**, (1), pp. 59–65

[3] Ngo, H.Q., Larsson, E.G., Marzetta, T.L.: 'Energy and spectral efficiency of very large multiuser MIMO systems', *IEEE Trans. Commun.*, 2013, **61**, (4), pp. 1436–1449

[4] Araujo, D.C., Maksymyuk, T., de Almeida, A.L., *et al.*: 'Massive MIMO: survey and future research topics', *IET Commun.*, 2016, **10**, (15), pp. 1938–1946

[5] Jose, J., Ashikhmin, A., Marzetta, T.L., *et al.*: 'Pilot contamination problem in multi-cell TDD systems'. Proc. IEEE Int. Symp. on Information Theory (ISIT), Seoul, Korea, 2009, pp. 2184–2188

[6] Gong, Z., Li, C., Jiang, F.: 'Pilot contamination mitigation strategies in massive MIMO systems', *IET Commun.*, 2017, **11**, (16), pp. 2403–2409

[7] Ali, S., Chen, Z., Yin, F.: 'Eradication of pilot contamination and zero forcing precoding in the multi-cell TDD massive MIMO systems', *IET Commun.*, 2017, **11**, (13), pp. 2027–2034

[8] Zhao, J., Ni, S., Gong, Y., *et al.*: 'Pilot contamination reduction in TDD-based massive MIMO systems', *IET Commun.*, 2019, **13**, (10), pp. 1425–1432

[9] Fernandes, F., Ashikhmin, A., Marzetta, T.L.: 'Inter-cell interference in noncooperative TDD large scale antenna systems', *IEEE J. Sel. Areas Commun.*, 2013, **31**, (2), pp. 192–201

[10] Hoydis, J., Ten-Brink, S., Debbah, M.: 'Massive MIMO in the UL/DL of cellular networks: how many antennas do we need?', *IEEE J. Sel. Areas Commun.*, 2013, **31**, (2), pp. 160–171

[11] Yin, H., Gesbert, D., Filippou, M., *et al.*: 'A coordinated approach to channel estimation in large-scale multiple-antenna systems', *IEEE J. Sel. Areas Commun.*, 2013, **31**, (2), pp. 264–273

[12] Ma, J., Ping, L.: 'Data-aided channel estimation in large antenna systems'. Proc. IEEE Int. Conf. on Communications (ICC), Sydney, Australia, 2014, pp. 4626–4631

[13] Li, L., Ashikhmin, A., Marzetta, T.: 'Pilot contamination precoding for interference reduction in large scale antenna systems'. Proc. IEEE 51st Annual Allerton Conf. on Communication, Control, and Computing, Monticello, Illinois, USA, 2013, pp. 226–232

[14] Fan, J., Li, W., Zhang, Y.: 'Pilot contamination mitigation by fractional pilot reuse with threshold optimization in massive MIMO systems', *Digit. Signal Process.*, 2018, **78**, pp. 197–204

[15] AlKhaled, M., Alsusa, E.: 'Impact of pilot sequence contamination in massive MIMO systems', *IET Commun.*, 2017, **11**, (13), pp. 2005–2011

[16] Peken, T., Vanhoy, G., Bose, T.: 'Blind channel estimation for massive MIMO', *Analog Integr. Circuits Signal Process.*, 2017, **91**, (2), pp. 257–266

[17] Amiri, E., Mueller, R., Gerstacker, W.: 'Blind pilot decontamination in massive MIMO by independent component analysis'. Proc. IEEE Globecom Workshops, Singapore, 2017, pp. 1–5

[18] Hu, D., He, L., Wang, X.: 'Semi-blind pilot decontamination for massive MIMO systems', *IEEE Trans. Wirel. Commun.*, 2016, **15**, (1), pp. 525–536

[19] Alwakeel, A.S., Mehana, A.H.: 'Semi-blind channel estimation and interference alignment for massive MIMO network'. Proc. IEEE Global Communications Conf. (GLOBECOM), Singapore, 2017, pp. 1–6

[20] Mahyiddin, W.A.W.M., Martin, P.A., Smith, P.J.: 'Performance of synchronized and unsynchronized pilots in finite massive MIMO systems', *IEEE Trans. Wirel. Commun.*, 2015, **14**, (12), pp. 6763–6776

[21] Pitarokoilis, A., Björnson, E., Larsson, E.G.: 'On the effect of imperfect timing synchronization on pilot contamination'. Proc. IEEE Int. Conf. on Communications (ICC), Paris, France, 2017, pp. 1–6

[22] Zou, X., Jafarkhani, H.: 'Asynchronous channel training in multi-cell massive MIMO', 2017, arXiv preprint arXiv:171103197

[23] Rekik, O., Ladaycia, A., Abed-Meraim, K., *et al.*: 'Performance bounds analysis for semi-blind channel estimation with pilot contamination in massive MIMO-OFDM systems'. Proc. IEEE 26th European Signal Processing Conf. (EUSIPCO), Rome, Italy, 2018, pp. 1267–1271

[24] Ladaycia, A., Mokraoui, A., Abed-Meraim, K., *et al.*: 'Performance bounds analysis for semi-blind channel estimation in MIMO-OFDM communications systems', *IEEE Trans. Wirel. Commun.*, 2017, **16**, (9), pp. 5925–5938

[25] Cho, Y.S., Kim, J., Yang, W.Y., *et al.*: '*MIMO-OFDM wireless communications with MATLAB*' (John Wiley & Sons, Hoboken, New Jersey, USA, 2010)

[26] Marzetta, T.L.: 'How much training is required for multiuser MIMO?'. Proc. IEEE 40th Asilomar Conf. on Signals, Systems and Computers (ACSSC), Pacic Grove, California, USA, 2006, pp. 359–363

[27] Caire, G., Jindal, N., Kobayashi, M., *et al.*: 'Multiuser MIMO achievable rates with downlink training and channel state feedback', *IEEE Trans. Inf. Theory*, 2010, **56**, (6), pp. 2845–2866

[28] Kay, S.M.: '*Fundamentals of statistical signal processing, volume I: estimation theory (v. 1)*' (PTR Prentice-Hall, Englewood Cliffs, 1993)

[29] Menni, T., Chaumette, E., Larzabal, P., *et al.*: 'New results on deterministic Cramér–Rao bounds for real and complex parameters', *IEEE Trans. Signal Process.*, 2012, **60**, (3), pp. 1032–1049

[30] Berriche, L., Abed-Meraim, K.: 'Stochastic Cramér-Rao bounds for semi-blind MIMO channel estimation'. Proc. IEEE 4th Int. Symp. on Signal Processing and Information Technology (ISSPIT), Rome, Italy, 2004, pp. 119–122

[31] Abeida, H., Delmas, J.P.: 'Gaussian Cramér-Rao bound for direction estimation of noncircular signals in unknown noise fields', *IEEE Trans. Signal Process.*, 2005, **53**, (12), pp. 4610–4618

[32] Omar, S.M., Slock, D.T., Bazzi, O.: 'Bayesian and deterministic CRBs for semi-blind channel estimation in SIMO single carrier cyclic prefix systems'. Proc. IEEE 22nd Int. Symp. on Personal Indoor and Mobile Radio Communications (PIMRC), Toronto, Ontario, Canada, 2011, pp. 1682–1686

[33] Abed-Meraim, K., Loubaton, P., Moulines, E.: 'A subspace algorithm for certain blind identification problems', *IEEE Trans. Inf. Theory*, 1997, **43**, (2), pp. 499–511

[34] Abed-Meraim, K., Qiu, W., Hua, Y.: 'Blind system identification', *Proc. IEEE*, 1997, **85**, (8), pp. 1310–1322

[35] Comon, P.: 'Independent component analysis, a new concept?', *Signal Process.*, 1994, **36**, (3), pp. 287–314

[36] Ladaycia, A., Mokraoui, A., Abed-Meraim, K., *et al.*: 'Toward green communications using semi-blind channel estimation'. Proc. IEEE 25th European Signal Processing Conf. (EUSIPCO), Greek island of Kos, Greece, 2017, pp. 2254–2258

[37] Bouguen, Y., Hardouin, E., Wolff, F.X.: '*LTE pour les reseaux 4G*' (Editions Eyrolles, Paris, France, 2012)